A Virtual Fixture Adaptation Strategy for MIRS Dissection Tasks

M. Selvaggio[1], G. A. Fontanelli[1], F. Ficuciello[1], L. Villani[1], and B. Siciliano[1]

[1] *Department of Information Technology and Electrical Engineering, University of Naples "Federico II"*

[1]mario.selvaggio@unina.it

INTRODUCTION

Shared-control techniques applied to robotic surgical interventions allow reducing the surgeon's mental workload, increasing the operative precision and/or decreasing the task completion time. Among these techniques, virtual fixtures (VFs) has been identified as one of the most promising approaches in robotic surgery [1]. VFs are software generated constraints which restrict the motion of a robotic manipulator into predefined regions [2]. This technique, although being very effective, is very often not practicable in unstructured surgical environments. In order to comply with the environmental deformation, the VF geometry and its constraint enforcement parameters need to be online adapted [3]. This paper proposes a strategy for an effective use of VF assistance in minimally invasive robotic surgical tasks. Passivity of the overall system is guaranteed by using energy tanks passivity-based control [4]. The proposed method is validated through experiments on the da Vinci Research Kit (dVRK).

MATERIALS AND METHODS

VFs are displayed to the operator through guidance forces applied to the master device of the teleoperation system. The n degree-of-freedom (DoF) manipulator controlled according to an impedance/admittance scheme exhibits the following Cartesian space dynamics

$$\boldsymbol{M}\ddot{\tilde{\boldsymbol{x}}} + \boldsymbol{D}\dot{\tilde{\boldsymbol{x}}} = \boldsymbol{f}_{\mathrm{h}} + \boldsymbol{f}_{\mathrm{vf}}(\cdot), \tag{1}$$

where $\tilde{\boldsymbol{x}} = (\boldsymbol{x}_{\mathrm{d}} - \boldsymbol{x})$ with $\boldsymbol{x} \in \mathbb{R}^r$ being the task space variable, and $\boldsymbol{x}_{\mathrm{d}}$ its desired value, $\boldsymbol{M} \in \mathbb{R}^{r\times r}$ and $\boldsymbol{D} \in \mathbb{R}^{r\times r}$ are fixed, diagonal and positive definite inertia and damping matrices, respectively, $\boldsymbol{f}_{\mathrm{h}} \in \mathbb{R}^r$ is the external force applied by an interacting user and $\boldsymbol{f}_{\mathrm{vf}}(\cdot)$ is the additional VF force.

A. Virtual Fixtures

A guidance VF exhibits attractive behavior towards a desired geometrical path. The simplest constraint enforcement method consists in applying a spring-damper like force. In the linear case this can be defined as follows

$$\boldsymbol{f}_{\mathrm{vf}}(\tilde{\boldsymbol{x}}, \dot{\tilde{\boldsymbol{x}}}) = -\boldsymbol{K}_{\mathrm{vf}}\tilde{\boldsymbol{x}} - \boldsymbol{D}_{\mathrm{vf}}\dot{\tilde{\boldsymbol{x}}}, \tag{2}$$

where $\boldsymbol{K}_{\mathrm{vf}} \in \mathbb{R}^{r\times r}$ and $\boldsymbol{D}_{\mathrm{vf}} \in \mathbb{R}^{r\times r}$ are properly designed diagonal and positive definite matrices and $\boldsymbol{x}_{\mathrm{d}}$ is the set-point belonging to the constraint geometry having minimum distance from $\boldsymbol{x}$. An impedance controlled manipulator (1), endowed with VF control forces defined in (2), exhibits a closed-loop behavior that can be described by

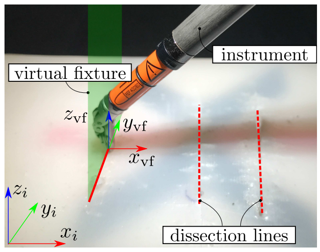

Fig. 1. VF adaptation experimental setup.

$$\boldsymbol{M}\ddot{\tilde{\boldsymbol{x}}} + \hat{\boldsymbol{D}}\dot{\tilde{\boldsymbol{x}}} + \boldsymbol{K}_{\mathrm{vf}}\tilde{\boldsymbol{x}} = \boldsymbol{f}_{\mathrm{h}}, \tag{3}$$

where $\hat{\boldsymbol{D}} = \boldsymbol{D} + \boldsymbol{D}_{\mathrm{vf}}$. To limit the VF spatial influence we adopt a non linear stiffness profile $\boldsymbol{K}_{\mathrm{vf}}$ designed as follows

$$k_{\mathrm{vf}}(\tilde{x}) = \beta(\tilde{x})K_{\mathrm{max}}, \tag{4}$$

where $\beta(\tilde{x}, t)$ is a stiffness shaping function and K_{max} is the predefined maximum stiffness value. For each task space variable $\beta(\tilde{x})$ is mathematically described by

$$\beta(\tilde{x}) = \begin{cases} 0 & \text{if } |\tilde{x}| \geq l \\ \frac{1}{2}\left(1 + \cos\left(\frac{\pi(|\tilde{x}| - d)}{l - d}\right)\right) & \text{otherwise} \\ 1 & \text{if } |\tilde{x}| \leq d \end{cases} \tag{5}$$

where l is the distance at which the VF attractive action vanishes completely and d is the threshold distance value inside which the stiffness perceived is K_{max}.

B. Virtual Fixture Adaptation

Our aim is to design a system that adapts the VF pose following a human-in-the-loop approach. The strategy consists in detecting interaction points at the slave side and use these to update the VF desired reference frame.

We use the classical least-squares minimization methods to fit a predefined geometry (without loss of generality we consider a vertical plane) onto the set of points. This current VF pose is adapted online by using a simple proportional control law defined on the pose error. In grater details, let $\mathcal{F}_{\mathrm{vf,d}}$ and $\mathcal{F}_{\mathrm{vf}}$ be the desired and current VF frames, the position error can be defined as

$$\boldsymbol{e}_P = \boldsymbol{O}_{\mathrm{vf,d}} - \boldsymbol{O}_{\mathrm{vf}} \tag{6}$$

where $\boldsymbol{O}_{\mathrm{vf,d}}$ and $\boldsymbol{O}_{\mathrm{vf}} \in \mathbb{R}^3$ denote the $\mathcal{F}_{\mathrm{vf,d}}$ and $\mathcal{F}_{\mathrm{vf}}$ origins, respectively. The proportional control law allows obtaining the following VF dynamics

$$\dot{\boldsymbol{O}}_{\mathrm{vf}} = -\boldsymbol{\Lambda}_p \boldsymbol{e}_P \qquad \boldsymbol{\Lambda}_p > 0, \tag{7}$$

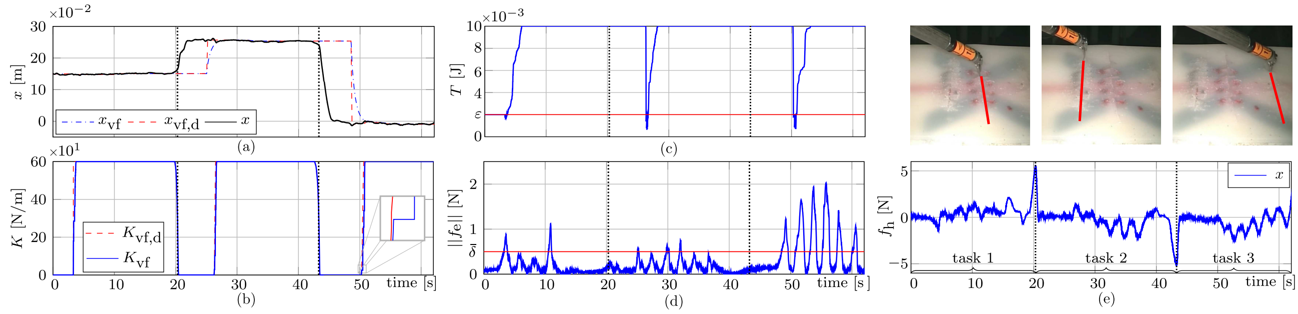

Fig. 2. VF pose adaptation experiment. Time histories of: (a) VF and tool central point pose along the x direction; (b) desired and current stiffness value; (c) energy tank level; (d) slave interaction force; (e) human operator estimated force on the master side.

that exponentially drives $\boldsymbol{O}_{\mathrm{vf}}$ to the desired value $\boldsymbol{O}_{\mathrm{vf,d}}$.

C. Passivity

To preserve the passivity of the resulting variable stiffness system we use the energy tanks-based approach. The extended system dynamics can be rewritten as follows

$$\begin{cases} \boldsymbol{M}\ddot{\tilde{\boldsymbol{x}}} + \hat{\boldsymbol{D}}\dot{\tilde{\boldsymbol{x}}} + \boldsymbol{K}_{\mathrm{vf}}\tilde{\boldsymbol{x}} = \boldsymbol{f}_{\mathrm{h}} \\ \dot{\boldsymbol{K}}_{\mathrm{vf}} = \alpha\left(\boldsymbol{\Lambda}_k\left(\boldsymbol{K}_{\mathrm{vf,d}} - \boldsymbol{K}_{\mathrm{vf}}\right) + \dot{\boldsymbol{K}}_{\mathrm{vf,d}}\right) \\ \dot{z} = \frac{\varphi}{z}\dot{\tilde{\boldsymbol{x}}}^{\mathrm{T}}\hat{\boldsymbol{D}}\dot{\tilde{\boldsymbol{x}}} - \frac{\gamma}{z}\frac{1}{2}\tilde{\boldsymbol{x}}^{\mathrm{T}}\dot{\boldsymbol{K}}_{\mathrm{vf}}\tilde{\boldsymbol{x}} \end{cases}, \tag{8}$$

where $\boldsymbol{\Lambda}_k \in \mathbb{R}^{r\times r}$ is a diagonal and positive definite matrix containing the stiffness tracking control parameter, $\alpha \in \{0,1\}$ is a variable used to activate/deactivate the stiffness variation in case of passivity violation, z is the state of the tank, φ and $\gamma \in \{0,1\}$ are control parameters. The master system, endowed with the energy tank, has the following energy function

$$\mathcal{H} = H + T = \frac{1}{2}\dot{\tilde{\boldsymbol{x}}}^{\mathrm{T}}\boldsymbol{M}\dot{\tilde{\boldsymbol{x}}} + \frac{1}{2}\tilde{\boldsymbol{x}}^{\mathrm{T}}\boldsymbol{K}_{\mathrm{vf}}\tilde{\boldsymbol{x}} + \frac{1}{2}z^2, \tag{9}$$

whose time derivative is given by

$$\dot{\mathcal{H}} = \dot{H} + \dot{T} = \dot{\tilde{\boldsymbol{x}}}^{\mathrm{T}}\boldsymbol{M}\ddot{\tilde{\boldsymbol{x}}} + \tilde{\boldsymbol{x}}^{\mathrm{T}}\boldsymbol{K}_{\mathrm{vf}}\dot{\tilde{\boldsymbol{x}}} + \frac{1}{2}\tilde{\boldsymbol{x}}^{\mathrm{T}}\dot{\boldsymbol{K}}_{\mathrm{vf}}\tilde{\boldsymbol{x}} + z\dot{z} \tag{10}$$

which, evaluated along the system trajectories, becomes

$$\dot{\mathcal{H}} = \dot{\tilde{\boldsymbol{x}}}^{\mathrm{T}}\boldsymbol{f}_{\mathrm{h}} - (1-\varphi)\,\dot{\tilde{\boldsymbol{x}}}^{\mathrm{T}}\hat{\boldsymbol{D}}\dot{\tilde{\boldsymbol{x}}} + (1-\gamma)\,\frac{1}{2}\tilde{\boldsymbol{x}}^{\mathrm{T}}\dot{\boldsymbol{K}}_{\mathrm{vf}}\tilde{\boldsymbol{x}}. \tag{11}$$

By defining the following control laws for α, φ and γ

$$\alpha = \begin{cases} 0 & \text{if } T \le \varepsilon \;\&\; \dot{\boldsymbol{K}}_{\mathrm{vf}} > 0 \\ 1 & \text{otherwise} \end{cases} \qquad \gamma = \begin{cases} \varphi & \text{if } \dot{\boldsymbol{K}}_{\mathrm{vf}} < 0 \\ 1 & \text{otherwise} \end{cases} \tag{12}$$
$$\varphi = \begin{cases} 1 & \text{if } T \le \bar{T} \\ 0 & \text{otherwise} \end{cases}$$

the system in (8) is passive with respect to the input-output pair $(\boldsymbol{f}_{\mathrm{h}}, \dot{\tilde{\boldsymbol{x}}})$ with storage function (9). $\bar{T}$ and ε in (12) are the upper and lower thresholds for the tank energy, respectively.

RESULTS

The proposed adaptation strategy is evaluated executing multiple dissection tasks in spatially separated regions (see Fig. 1). In the considered case (planar VF), the fitting strategy reduces to a linear regression problem. The desired VF reference frame is fitted using the last fifty recorded interaction poses of the slave robot with the environment.

Fig. 2 contains the results of a performed experiment. The graph 2(a) contains the VF desired and current pose together with the robot tool central point position, while in Fig. 2(b) the user perceived stiffness is shown. The energy tank passivity-based control ensures a passive behavior by implementing the change in stiffness only when sufficient tank energy is at disposal. This is evident looking at Figs. 2(b) and 2(c). In particular, the stiffness is kept constant (*i.e.* $\dot{K}_{\mathrm{vf}} = 0$) when the tank is empty, thus not introducing discontinuities in the system. Fig. 2(b) contains a focus around 50 s that emphasizes this behavior.

Fig. 2(d) shows the interaction force norm measured at the slave side using an ATI nano 17 F/T sensor together with the chosen threshold $\bar{\delta} = 0.5$ N used to discriminate between interaction and free motion.

Finally, looking at the master estimated forces in Fig. 2(e), it can be noticed that relatively high forces (≈ 5 N) are only applied at the task switching.

CONCLUSIONS AND DISCUSSION

In this work we have introduced and experimentally validated the use of adaptive VF for dissection tasks in MIRS. An adaptation strategy is proposed together with a suitable nonlinear stiffness profile for guidance VF. Passivity of the system is preserved by using energy-tank passivity-based control.

Future works will explore the use of online user-defined VF geometries and generalization of the proposed methods to other surgical procedures. In addition, the use of shared control in surgical operations will be further assessed by surgeons user studies.

REFERENCES

[1] N. Enayati, E. D. Momi, and G. Ferrigno, “Haptics in robot-assisted surgery: Challenges and benefits,” *IEEE Rev. Biomed. Eng.*, vol. 9, pp. 49–65, 2016.

[2] S. A. Bowyer, B. L. Davies, and F. R. y Baena, “Active constraints/virtual fixtures: A survey,” *IEEE Trans. Robot.*, vol. 30, no. 1, pp. 138–157, 2014.

[3] D. Zhang, Q. Zhu, J. Xiong, and L. Wang, “Dynamic virtual fixture on the euclidean group for admittance-type manipulator in deforming environments,” *Biomed Eng Online*, vol. 13, no. 1, p. 51, 2014.

[4] F. Ferraguti, C. Secchi, and C. Fantuzzi, “A tank-based approach to impedance control with variable stiffness,” in *IEEE Int. Conf. on Robotics and Automation*, 2013, pp. 4948–4953.

[5] M. Selvaggio, G. A. Fontanelli, F. Ficuciello, L. Villani, and B. Siciliano, “Passive virtual fixtures adaptation in minimally invasive robotic surgery,” *IEEE Robotics and Automation Letters*, vol. 3, no. 4, pp. 3129–3136, Oct 2018.